Geotechnical and Geophysical Site Characterisation 5 – Lehane, Acosta-Martínez & Kelly (Eds)

Simulation of the cone penetration test: discrete and continuum approaches

A. Gens, M. Arroyo, J. Butlanska & L. Monforte
Department of Civil and Environmental Engineering, Universitat Politècnica de Catalunya, Barcelona, Spain

J.M. Carbonell
International Centre for Numerical Methods in Engineering (CIMNE), Barcelona, Spain

M. Ciantia, C. O'Sullivan
Department of Civil and Environmental Engineering, Imperial College, London, UK

ABSTRACT: The paper presents the modelling of the cone penetration test using two procedures: a discrete approach and a continuum approach. The discrete approach is based on the Discrete Element Method where a granular material is represented by an assembly of separate particles. Cone penetration has been simulated for both uncrushable and crushable sands. For the continuum approach, the Particle Finite Element Method has been adapted in order to overcome the difficulties posed by the occurrence of large displacements as well as by the geometrical, material and contact nonlinearities of the problem. Both single phase and two-phase (coupled hydromechanical) formulations have been developed and applied. Although not exempt of problems, both approaches yield realistic results leading to the possibility of a closer examination and an enhanced understanding of the mechanisms underlying cone penetration.

1 INTRODUCTION

Penetration problems are widespread in geotechnical engineering. Among them, cone penetration is one the prime means of soil investigation but its interpretation remains largely empirical especially for sands (Mayne 2007, Schnaid 2009); theoretical approaches are more advanced for clays (e.g. Randolph 2004). A more rational interpretation may benefit from appropriate modelling although it must be recognized that significant challenges arise when numerical analyses of penetration problems are undertaken. Those types of problems involve large deformations as well as geometrical and contact nonlinearities. Also, complex constitutive laws are generally required to represent adequately the mechanical behaviour of geotechnical materials.

The paper presents a brief summary of some recent work carried out by our group concerning the modelling of penetration problems and, more specifically, the simulation of cone penetration tests. Two approaches have been pursued: discrete modelling and continuum modelling. Granular soils have been modelled by an assembly of distinct particles using the Discrete Element Modelling (DEM). This approach is not practicable in the case of fine-grained materials where a continuum analysis has been favoured. The Particle Finite Element Method (PFEM) has been employed as the preferred numerical technique for this approach.

2 DISCRETE MODELLING

2.1 *General*

The use of the Discrete Element Method (DEM) to model the mechanical behaviour of granular materials has certainly important limitations bus also a considerable number of advantages (O'Sullivan, 2011). Among the limitations are the generally oversimplified geometrical representation of the particles (often assumed to be spheres) and the need to scale up their size, especially in boundary value problems such as the cone penetration analyses. In spite of this scaling, the resulting calculations are computationally intensive if a sufficiently representative number of particles are considered.

The main advantage is that large strains, displacements and rotations are readily accommodated in the analyses. Also, it is possible to bypass the need for quite sophisticated constitutive models for sands; instead only the contact law between pairs of individual particles are usually required. It should be noted, however, that there is considerable uncertainty over the precise form of those contact laws and their parameters are generally calibrated comparing the macroscopic response of a DEM model and the results of analogous laboratory tests.

First attempts to use DEM to simulate cone penetration tests (Huang & Ma 1994, Calvetti & Nova 2005, Jiang et al. 2006) used 2D elements (i.e. disks). Although undoubtedly useful, they fail however to provide a realistic representation of the kinematics of granular deformation. More representative results are obtained using 3D analyses although, so far, they have been limited to spherical shapes (Butlanska et al. 2010a, 2010b, Arroyo et al. 2011, Mcdowell et al. 2012, Lin &Wu 2012, Butlanska et al. 2013).

2.2 *Cone penetration modelling in crushable sands*

A strong motivation for this modelling work has been to explore the possibility to develop virtual calibration chambers, VCC (Arroyo et al. 2011). Analyses have been performed with the PFC3D code (Itasca 2010); the rotation of spheres has been inhibited in order to capture the limited rotation observed when non-spherical particles are involved. The necessary limitation of the number of particles employed in the analyses has required the adoption of results' filtering (to smooth the oscillation of cone resistance) and to account for chamber size effects, a requirement also necessary in the interpretation of the results form physical calibration chambers. Another importance difference with the physical system lies in the fact that the way of forming the specimens is quite different in the virtual and in the physical calibration chambers, leading to differences in initial fabric.

In spite of those difficulties, it has been possible to obtain good quantitative agreement between the results of the DEM analyses and the extensive set of data reported by Jamiolkowski et al. (2003). The tests were performed on Ticino sand, a medium-size silica sand with mostly sub-rounded grains. Because of the strength of the basic particle material, it was not necessary to account for grain crushing in the analyses. Figure 1 (Arroyo et al. 2011) shows the comparison for a number of tests covering relative densities form 60% to 90% and confining pressures from 40 to 400 kPa.

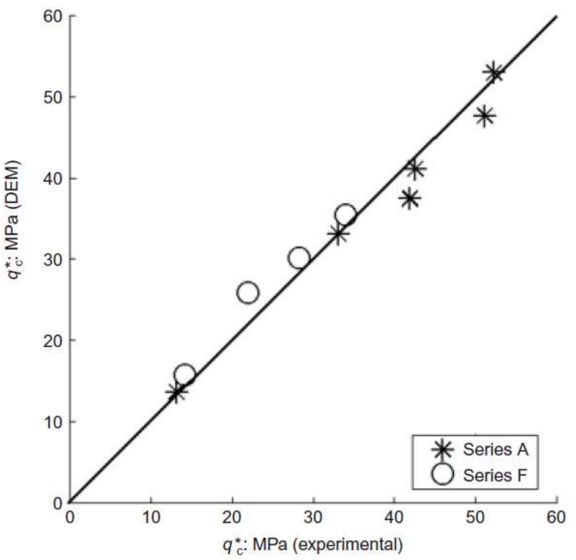

Figure 1. Comparison between corrected cone resistance from DEM and corrected cone resistance values from physical tests on Ticino sand.

One of the important advantages of using DEM is the possibility to perform observations not only at the microscale (individual particles and contacts) but also at the mesoscale (continuum stress-strain). The mesoscale is particularly useful as the observations have direct counterparts in continuum analysis (Butlanska et al., 2011, 2014).

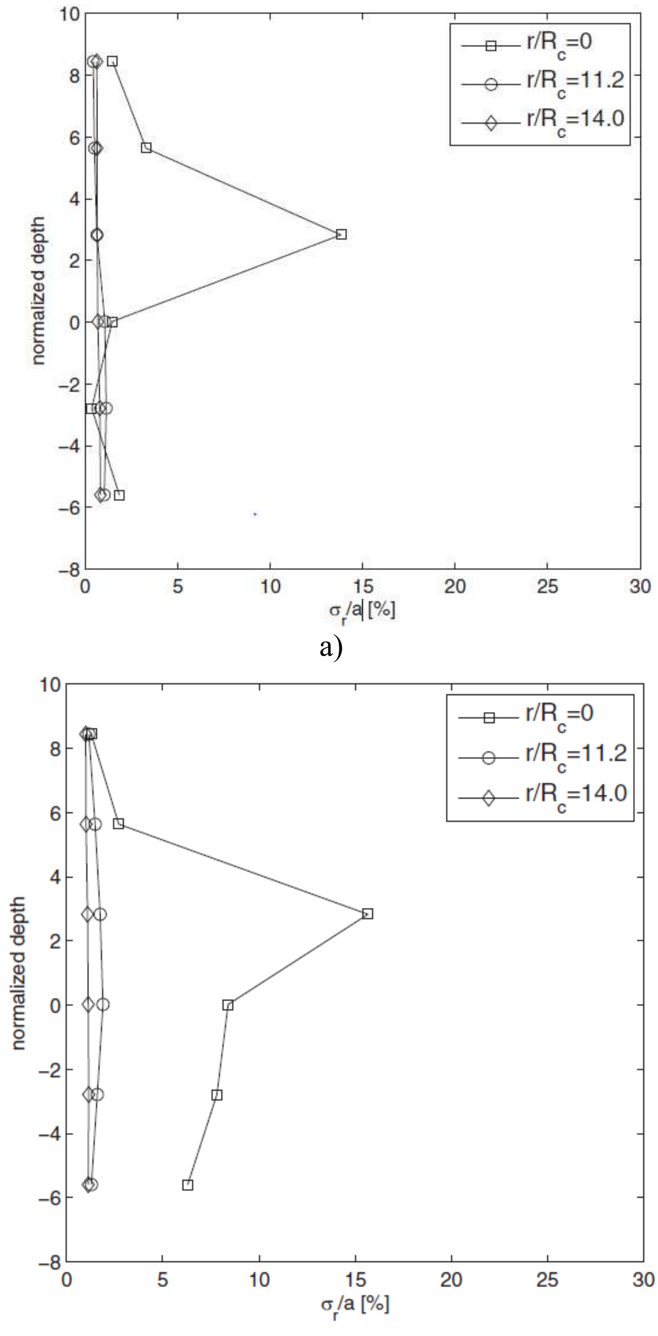

Figure 2. Distribution of radial stresses at different radial distances, r, normalized by cone radius, R_c. Stresses are normalized by cone resistance, a. Normalized depth 0 corresponds to the cone tip position. a) No lateral displacement condition (BC3). b) Constant radial stress condition (BC1)

As an example, Figure 2 shows the computed distribution of radial stress at different radial distances for a dense granular assembly under two different boundary conditions. The distributions close to the axis of the cone closely resemble the experimental observations obtained by Jardine et al. (2013) in a physical chamber. Indeed, as shown in Figure 3, the peak values computed from the DEM analyses follow the same quantitative trend as those obtained in the physical chamber tests.

It appears therefore, that in spite of its limitations, DEM analysis is capable to simulate satisfactorily many of the physical features of cone penetration in granular materials. In addition, it is possible to achieve an enhanced understanding of the underlying mechanisms when examining the results at the microscale and at the mesoscale.

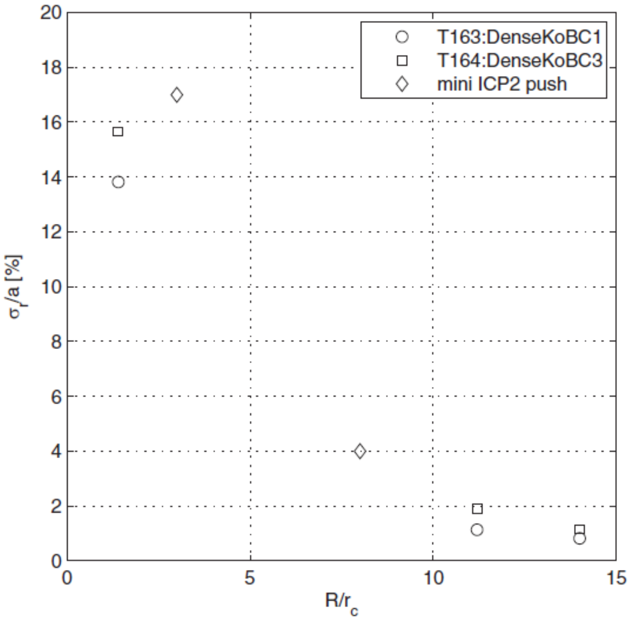

Figure 3. Peak values of normalized radial stress versus normalized radial distance (see caption of Figure 2). DEM results and physical chamber observations from Jardine et al. (2013).

2.3 *Cone penetration modelling in crushable sands*

Granular materials made up of weaker grains, such as calcareous sands, often exhibit significant particle crushing when subjected to high or even moderate stresses. It has been observed (e.g. Almeida et al. 1991) that the pattern of cone resistance increase with relative density is notably different in calcareous crushable sand compared to non-crushable silica sand. This difference results in difficulties when correlations developed for silica sands are applied to materials with crushable grains (Ahmed et al. 2014, Moss 2014). In this context, the application of DEM analysis is appealing because it allows isolating the effects of grain strength and crushability. It will be applied to an extreme case, reported by Wesley (2007), where the cone resistance was insensitive to relative density (Figure 4). The material is a volcanic pumice sand the grains of which are porous themselves.

To performed those analyses, it is necessary to extend the DEM formulation to account for the possibility of grain crushing. Two different approaches have been proposed: the use of multigrain aggregates (Cheng et al. 2003, Bolton et al. 2008) or a multigenerational approach (Marketos & Bolton 2009, Ben-Nun & Einav 2010, Bruchmüller et al. 2011) in which a single element breaks and it is replaced by a new generation of smaller grains.

Recently, an efficient formulation has been proposed, using the latter approach, that allows the performance of DEM analyses of boundary value problems in a reasonably economical manner (Ciantia et al. 2014, 2015). The main features of this approach can be summarized as follows: a particle failure criterion inspired by the analytical work of Russell & Muir Wood (2009) and Russell et al. (2009), a particle spawning procedure based on Apollonian packing and upscaling rules for particle strength and contact constant stiffness parameters for both linear and Hertzian contact laws. As in many multigenerational approaches, mass is not conserved after particle splitting but the missing mass of broken particles is allocated, during post-processing, to finer fractions according to a fractal distribution. In this way, it is possible to track evolving porosity and grain size distribution (GSD). Figure 5 shows the configuration of the spawned particles after the breakage of a single sphere. It has been shown (Ciantia et al. 2015) that this DEM formulation readily captures the macroscopic behaviour of highly crushable granular materials.

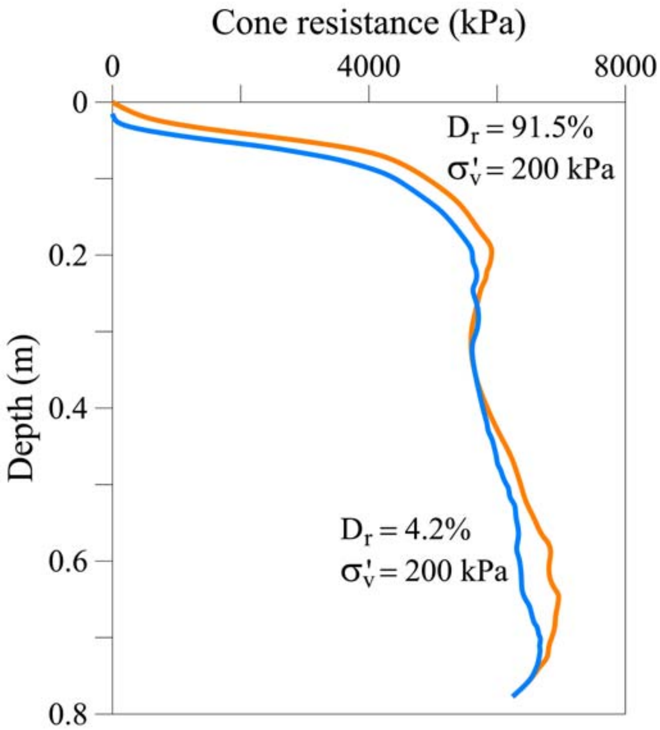

Figure 4. CPT results observed in cone penetration tests on pumice sand performed in a calibration chamber. (Wesley 2007).

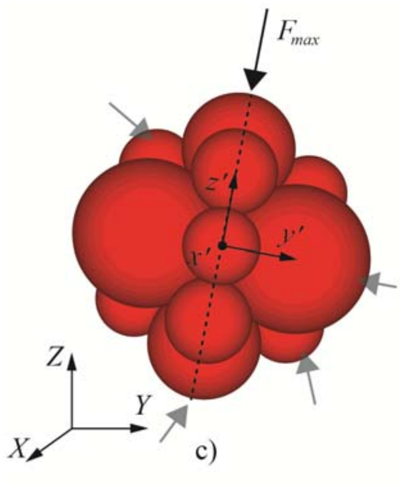

Figure 5. Apollonian configuration of the spawned particles after the breakage of a single sphere

The DEM model has been calibrated against oedometer and triaxial tests on the pumice sand used in the calibration chamber tests (Wesley 2007). For instance, Figure 6 shows the comparison with two oedometer tests performed at different densities. Grain size distributions were determined at various values of vertical stress. Figure 7 shows that the grain fragmentation procedure is able to follow successfully the evolution of the GSD during tests reaching a vertical stress of 8 MPa.

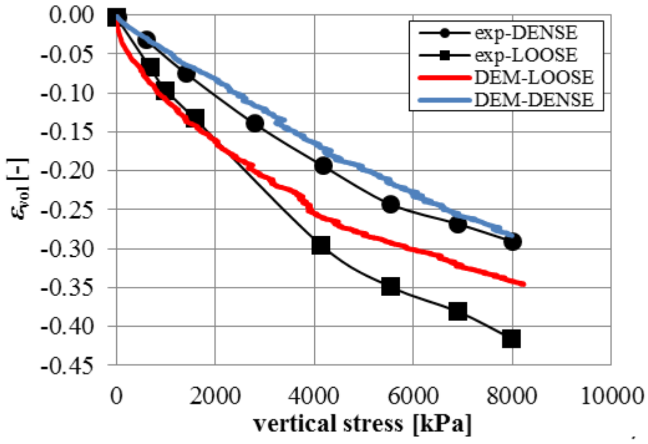

Figure 6. Observed and computed volumetric strain in oedometer tests on pumice sands.

The virtual calibration chamber (Figure 8) has been constructed with the same procedure employed for silica uncrushed sand (Arroyo et al. 2011) and a similar upscaling procedure for grains and cone has been used. The zero-strain radial lateral condition of the physical chamber was replicated by the model. Selected results of the DEM analyses are presented in Figure 9 where it is apparent that the cone penetration values are quite insensitive to the density of the sand, as observed in the physical experiments.

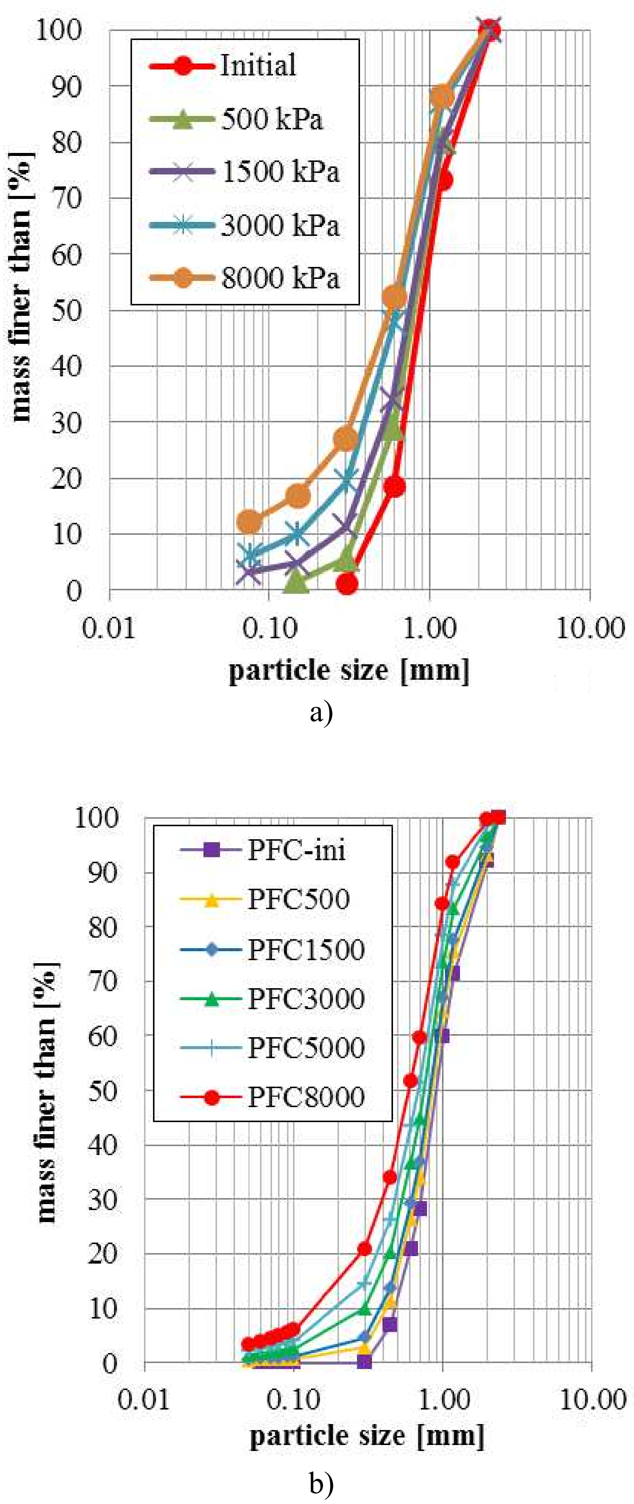

Figure 7. Evolution of grain size distribution in oedometer tests on pumice sand. a) Experimental observations, b) Computations

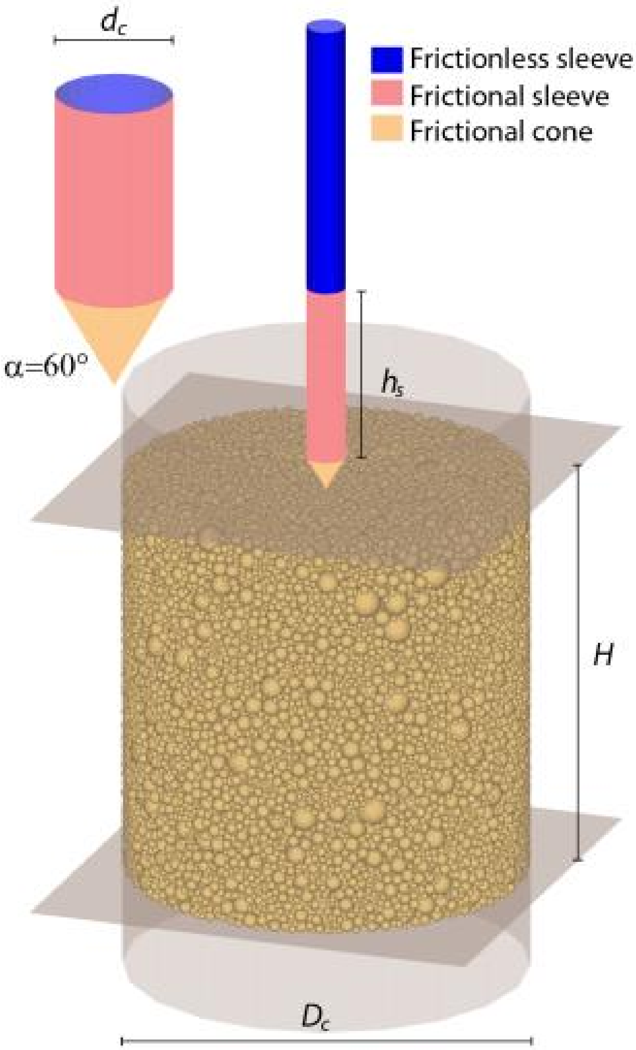

Figure 8. Virtual calibration chamber and cone

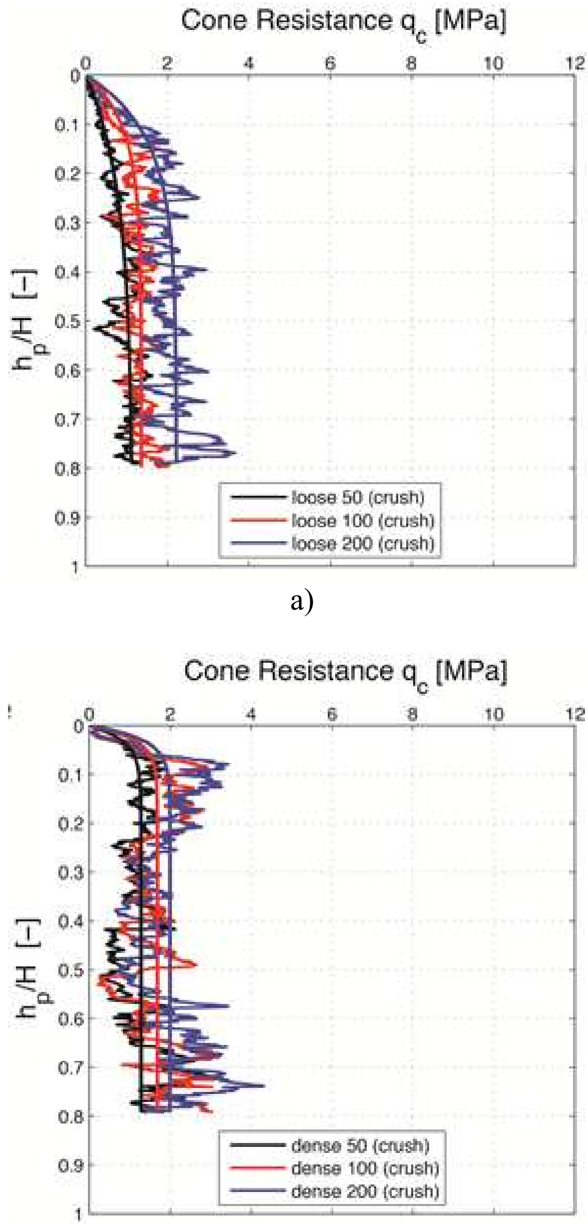

Figure 9. Computed cone resistance of simulated cone penetration tests on pumice sand at different stress values. a) Loose specimen, b) Dense specimen.

Parallel DEM calculations assuming uncrushable grains were also performed so that the effects of particle crushability could be readily identified. Results in terms of ratio of cone penetration resistance of uncrushable and crushable granular materials are collected in Figure 10. It can be noted that the pattern of variation with relative density agrees well with reported experimental results. No DEM results are available for densities below about 40% due to the difficulty of constructing very loose virtual specimens. In any case, it appears that the use of the new DEM formulation for crushable materials provides a good tool to further explore penetration problems in this type of materials. More information on this study is given in Ciantia et al. (2016).

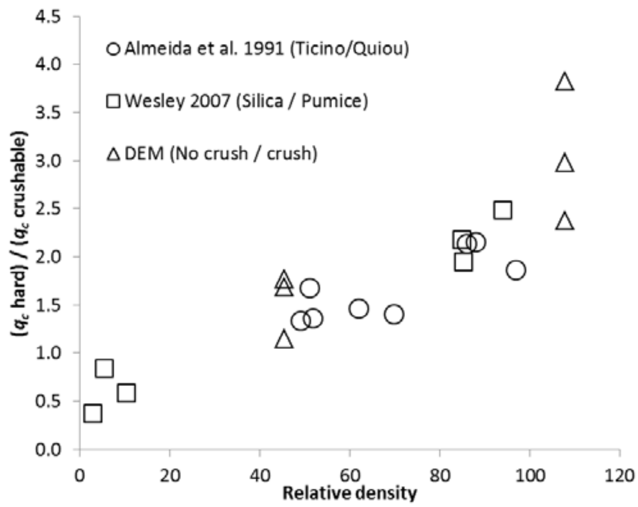

Figure 10. Effect of crushability on cone resistance for different relative densities. Experimental and DEM results.

3 CONTINUUM MODELLING

3.1 *General*

The continuum modelling of the cone penetration test has been performed using the Particle Finite Element Method, PFEM (Idelshon et al. 2004, Onate et al. 2004, Carbonell 2009).

The PFEM uses a Finite Element approximation to compute the movement of the particles within an updated Lagrangian framework. In this method particles and nodes coincide and the mesh is updated when required to prevent excessive distortions; Delaunay tessellation is used for this purpose. The mesh nodes are considered particles that carry mass and the state variables and, being particles, they can separate from the main domain giving rise to new boundaries. For this reasin, the Alpha Shape technique (Edelsbrunner & Mucke 1994) is used to identify the boundaries at every step of the analysis. Further refinements involve the addition/removing of particles depending on a characteristic distance and the formulation of the contact conditions via a penalty method. Although the method was initially developed for fluid-solid interaction problems, there have already been some applications to geotechnical problems (Carbonell et al. 2010, Zhang et al. 2013, 2015).

Figure 11 shows a scheme of the method that can be summarised in the following steps: i) A cloud of particles, C_n, is defined at a time $t=t_n$, ii) identify the boundaries defining the analysis domain, iii) discretize the domain with a finite element mesh, iv) solve the governing equations within a Lagrangian formulation and compute the state variables at the next updated configuration at t_{n+1}, v) move the nodes to the new position C_{n+1}, vi) go back to step i).

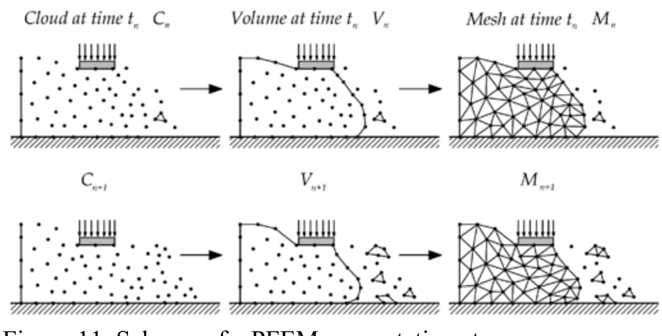

Figure 11. Scheme of a PFEM computation step

3.2 *Single phase formulation*

In a purely undrained case the soil can be considered as a single phase medium and only the linear momentum balance equation (equilibrium) needs to be solved. Accordingly, a total-stress Tresca constitutive model has been adopted to represent the soil whereas the tangential contact with the rigid cone has been simulated with a von Mises yield criterion. The analyses presented here have been performed with a rigidly index, I_r = 100. The geometry of the problem and the computation domain are shown in Figure 12.

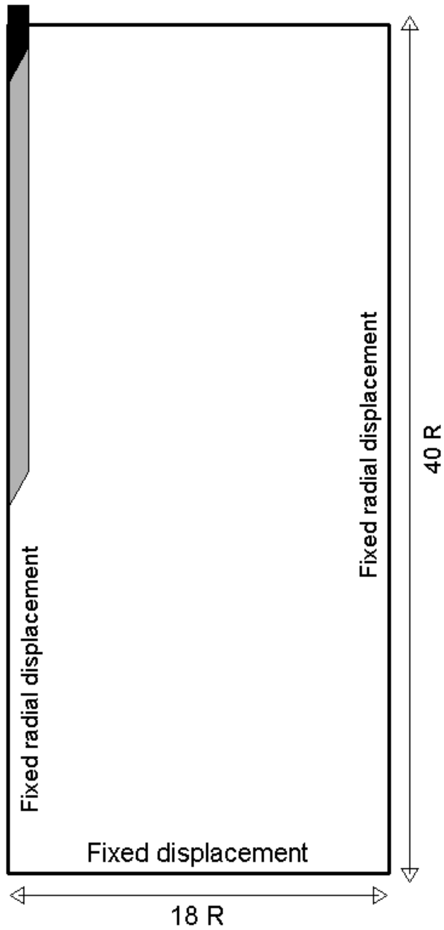

Figure 12. Geometry and computational domain of the PFEM analysis of cone penetration

The cone penetration analyses have been carried out using values of cone-soil adhesion ratio (α=adhesion/undrained shear strength) ranging from 0 to 0.7. The results in terms of cone penetration (normalized as cone factor N_{kt}) and friction sleeve resistance are plotted in Figure 13. As expected, the friction sleeve resistance coincides with the specified adhesion and the cone resistance increases modestly with the value of adhesion. Figure 14 shows more explicitly the variation of cone factor with the value of adhesion

3.3 *Two-phase formulation*

The PFEM formulation has been extended to deal with coupled hydromechanical problems so that the full range of partially drained conditions and consolidation problems for saturated soils can be examined. Consequently, the formulation requires the simultaneous solution of the equilibrium equation and of the water mass conservation. Now, the soil constitutive models can be expressed in terms of effective stresses.

Using this formulation, the problem of cone penetration has been analysed adopting Modified Cam clay as the constitutive model for the soil. An explicit finite deformation integration of the constitutive law is used following the procedure outlined in Monforte et al. (2015). Figure 15 shows the contours of total displacements at three stages of penetration: initial and at normalised penetration ratios (z/R) of 6 and 10. z is the penetration depth and R the cone radius. z/R= 10 corresponds to a steady state condition. The progress of the PFEM analysis is illustrated in Figure 16 where the evolution of the mesh during the calculation is presented. The refinement of the mesh of the soil domain directly affected by the penetration is apparent.

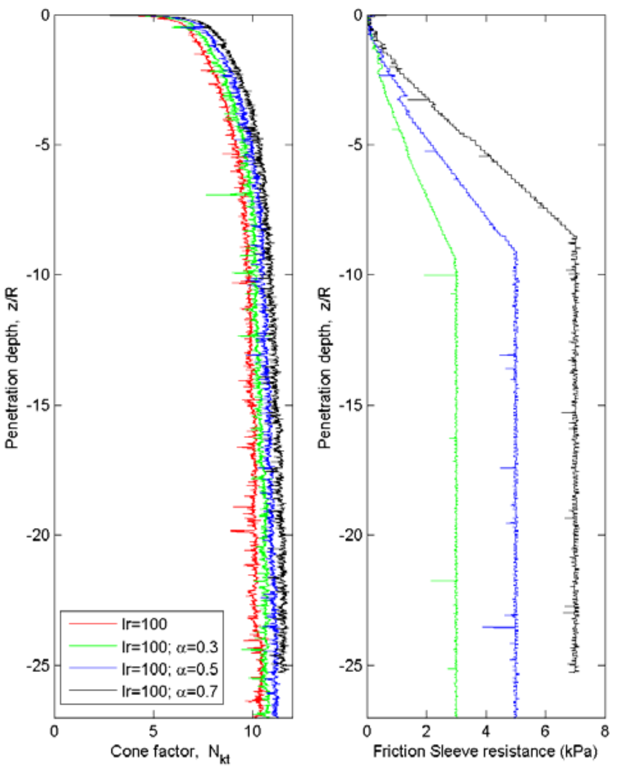

Figure 13. Cone factor and friction sleeve resistance for different values of adhesion computed with PFEM

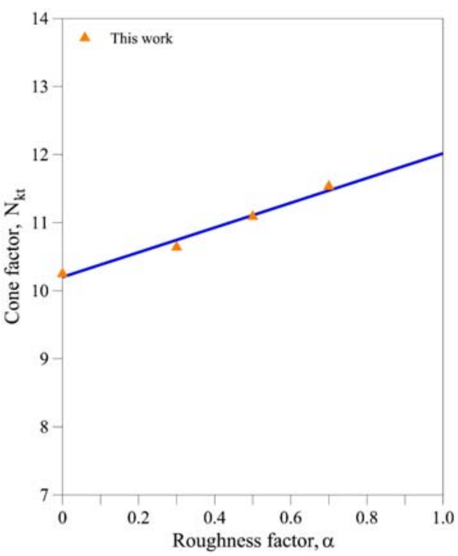

Figure 14. Variation of cone factor with adhesion, α

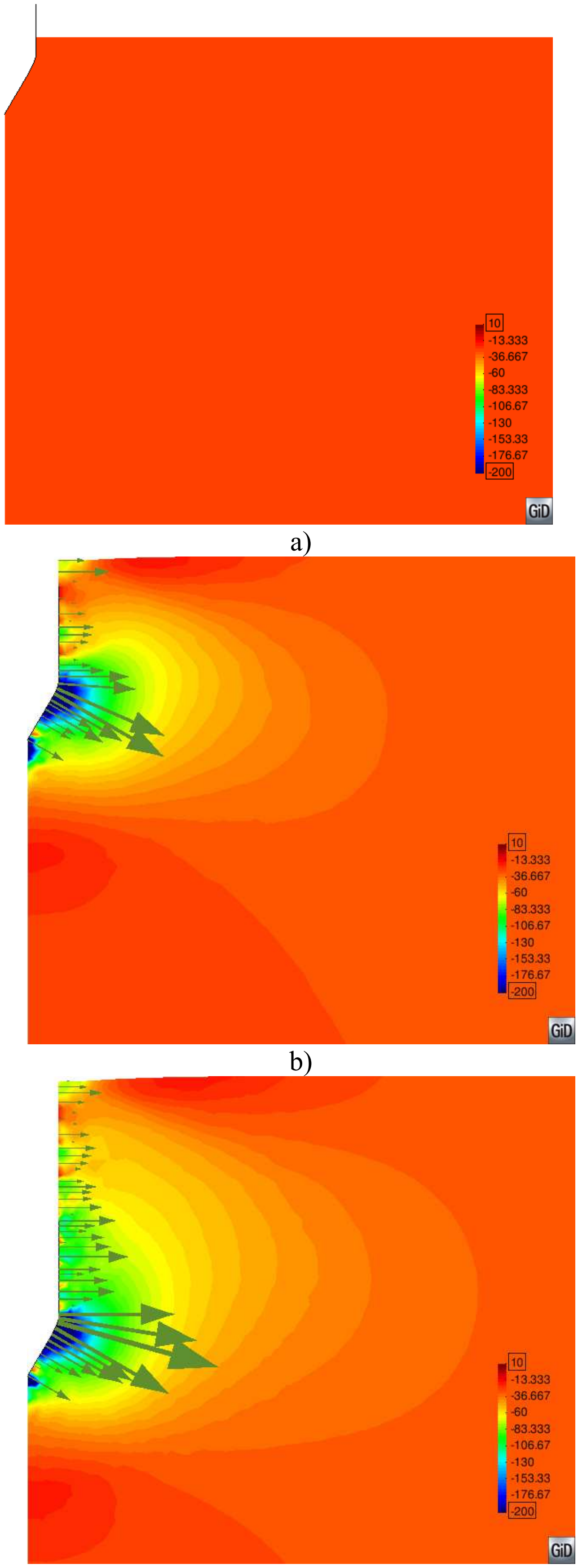

Figure 15. Total displacements during cone penetration. a) Initial, b) z/R=6, c) z/R=10. z: penetration depth and R: cone radius.

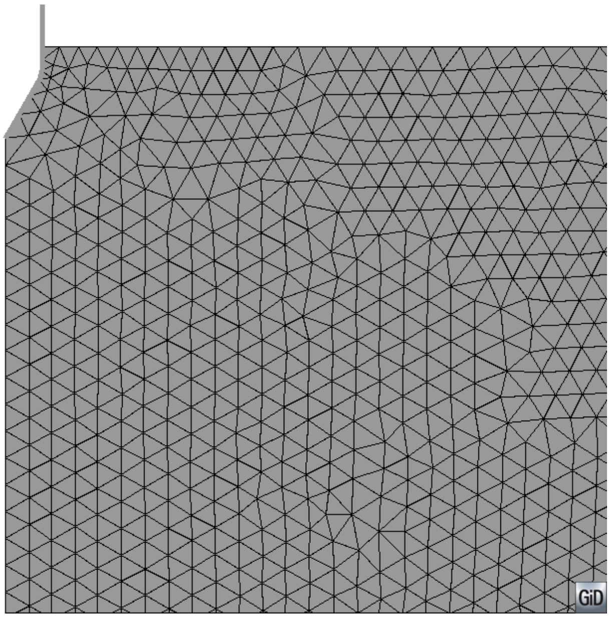

a)

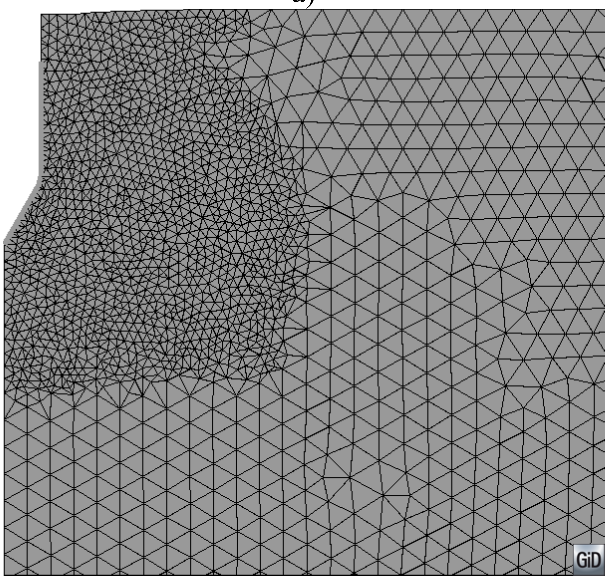

b)

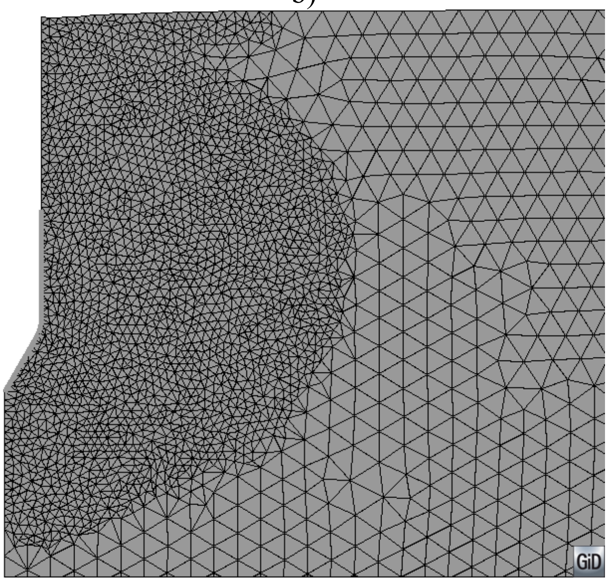

c)

Figure 16. Evolution of the PFEM mesh during cone penetration. a) Initial, b) z/R=6, c) z/R=10. z: penetration depth and R: cone radius.

Figure 17 presents the variation of cone resistance with penetration depth showing that a steady state condition has been reached. Some oscillations in the solution can be noted; they result from the incompressibility of the soil at critical state combined with the use of low-order elements in the mesh. To address this issue, mixed formulations have been recently developed (Monforte et al. 2016) that have proved very successful in overcoming this problem.

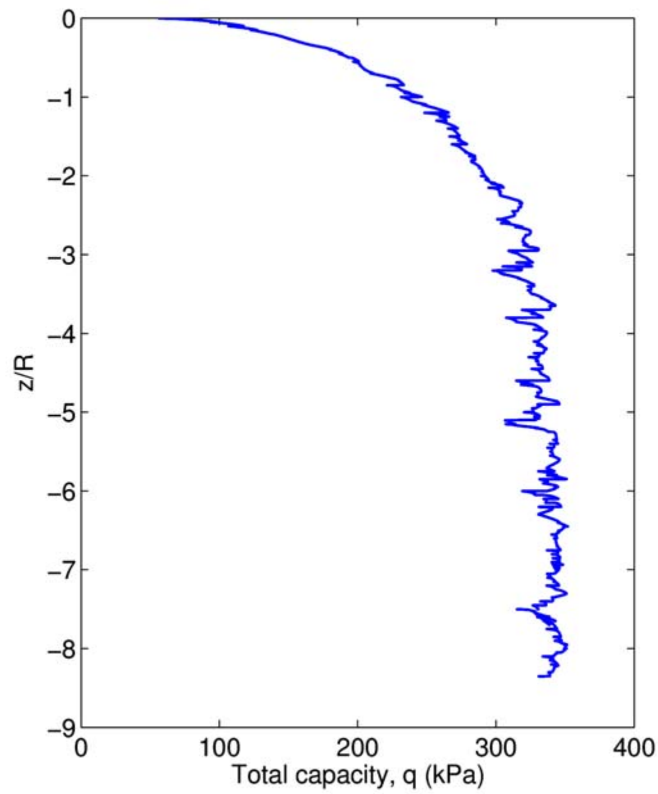

Figure 17. Variation of penetration resistance with depth. z: penetration depth and R: cone radius

4 CONCLUSIONS

Two different approaches have been presented for the modelling of the cone penetration test that attempt to overcome the considerable difficulties associated with the simulation of penetration problems, i.e. large displacements, large strains and rotations, severe domain distortion as well as geometrical, material and contact nonlinearities. Both the DEM and PFEM procedures have shown their capabilities in this context although some significant challenges and shortcomings remain. They constitute, however, areas of intense development and research that should lead to an increasingly realistic description of the process of cone penetration in all its complexity. Consequently, it can be envisaged that more rational-based procedures for the interpretation of the test should ensue or, at least, a better understanding of the mechanisms underlying cone penetration should be achieved.

5. ACKNOWLEDGEMENTS

The support of the Ministerio de Economía y Competividad of Spain through research grants BIA2011-27217 and BIA2014-59467-R is gratefully acknowledged.

6. REFERENCES

Ahmed, S. M., Agaiby, S. W. & Abdel-Rahman, A. H. 2014. A unified CPT–SPT correlation for non-crushable and crushable cohesionless soils. *Ain Shams Engineering Journal* 5: 63-73

Almeida, M., Jamiolkowski, M., & Peterson, R. 1991. Preliminary result of CPT tests in calcareous Quiou sand. *Proceedings of the International Symposium on Calibration Chamber Testing*: 41-53. New York: Elsevier.

Arroyo, M., Butlanska, J., Gens, A., Calvetti, F., & Jamiolkowski, M. 2011. Cone penetration tests in a virtual calibration chamber. *Géotechnique*, 61: 525-531.

Ben-Nun, O. & Einav, I. 2010. The role of self-organization during confined comminution of granular materials. *Phil. Trans. R. Soc.* A 368, No. 1910: 231–247.

Bolton, M. D., Nakata, Y. & Cheng, Y. P. 2008. Micro- and macro-mechanical behaviour of DEM crushable materials. *Géotechnique* 58 : 471–480.

Bruchmüller, J., Van Wachem, B. G. M., Gua, S. & Luo, K. H. 2011. Modelling discrete fragmentation of brittle particles. *Powder Technol.* 208: 731–739.

Butlanska, J., Arroyo, M., & Gens, A. 2010a. Size effects on a virtual calibration chamber. In T. Benz and S. Nordal (eds.), *Numerical methods in geotechnical engineering*: 225-230. CRC Press, Balkema.

Butlanska, J., Arroyo, M., & Gens, A. 2010b. Virtual calibration chamber CPT tests on Ticino sand. *Proceedings of the 2nd International Symposium on Cone Penetration Testing, CPT'10*: 217–224.

Butlanska, J., Arroyo, M., & Gens, A. 2013. 3D DEM simulations in sand. In Coutinho & Mayne (eds.), *Geotechnical and Geophysical Site Characterization*. 817- 824. London: Taylor & Francis.

Butlanska, J., Arroyo, M., Gens, A. & OSullivan, C. 2014. Multi-scale analysis of cone penetration (CPT) in a virtual calibration chamber. *Canadian Geotechnical Journal*. 51: 51-66.

Butlanska, J., OSullivan, C., Arroyo, M., & Gens, A. 2011. Mapping deformation during CPT in a virtual calibration chamber. *Proceedings of the International Symposium on Geomechanics and Geotechnics: From Micro to Macro*: 559–564. London: Taylor & Francis..

Calvetti, F., & Nova, R. 2005. Micro-macro relationships from DEM simulated element and in-situ tests. *Proc. 5th Int. Conf. Micromechanics of Granular Media: Powders and Grains 2005, Stuttgart*: 245–250.

Carbonell, J.M. 2009. *Modeling of ground excavation with the Particle Finite Element Method.* Ph.D. Thesis. Universitat Politècnica de Catalunya, Barcelona.

Carbonell J.M., Onate, E. & Suarez, B. 2010. Modeling of ground excavation with the Particle Finite Element Method. *Journal of Engineering Mechanics, ASCE*. 136: 455-463.

Cheng, Y. P., Nakata, Y. & Bolton, M. D. 2003. Discrete element simulation of crushable soil. *Géotechnique* 53: 633–641.

Ciantia, M. O., Arroyo, M., Butlanska, J. & Gens, A. 2014. DEM modelling of a double-porosity crushable granular material. In K. Soga et al. (Ed.), *Proc. Int. Symp. on Geomechanics from Micro to Macro*: 269-274. London: Taylor & Francis.

Ciantia, M. O., Arroyo, M., Butlanska, J. & Gens, A. 2016. DEM modelling of cone penetration test in a double-porosity crushable granular material. *Computers and Geotechnics*. 2016:109-127.

Ciantia, M. O., Arroyo, M., Calvetti, F. & Gens, A. 2015. An approach to enhance efficiency of DEM modelling of soils with crushable grains. *Géotechnique*. 65: 91–110.

Edelsbrunner, H. & Mucke, E.P. 1994. Three dimensional alpha shapes. *ACM Transaction on Graphics*, 13. 43-72.

Huang, A.-B. & Ma, M.Y. 1994. An analytical study of cone penetration tests in granular material. *Canadian Geotechnical Journal*,. 31: 91–103.

Idelsohn, S.R., Onate, E., Del Pin, F. 2004. The particle finite element method: a powerful tool to solve incompressible flows with free-surfaces and breaking waves. *Int J Numer Meth Eng.* 61:964–89.

Itasca. 2010. *Particle flow code in three dimensions: software manual.* Minnesota, USA.

Jamiolkowski, M., Lo Presti, D.C.F., & Manassero, M. 2003. Evaluation of relative density and shear strength of sands from CPT and DMT. *Soil behavior and soft ground construction. American Society of Civil Engineers*: 201–238.

Jardine, R.J., Zhu, B.T., Foray, P., & Yang, Z.X. 2013. Measurement of stresses around closed-ended displacement piles in sand. *Géotechnique*, 63: 1–17.

Jiang, M.J., Yu, H.-S., & Harris, D. 2006. Discrete element modelling of Deep penetration in granular soils. *International Journal for Numerical and Analytical Methods in Geomechanics*, 30: 335–361.

Lin, J., & Wu, W. 2012. Numerical study of miniature penetrometer in granular material by discrete element method. *Philosophical Magazine*. 92(28–30): 3474–3482.

Marketos, G., & Bolton, M. D. 2010. Flat boundaries and their effect on sand testing. *International Journal for numerical and analytical methods in geomechanics*, 34: 821-837

Mayne, P. W. 2007. In-situ test calibrations for evaluating soil parameters. In Tan et al. (ed.) *Characterisation and Engineering properties of Natural Soils*. 3: 1601–1652. London: Taylor & Francis.

Mcdowell, G.R., Falagush, O., & Yu, H.-S. 2012. A particle refinement method for simulating DEM of cone penetration testing in granular materials. *Géotechnique Letters*, 2: 141–147.

Monforte, L., Arroyo, M., Gens, A. & Carbonell, J.M., 2015. Explicit finite deformation stress integration of the elastoplastic constitutive equations. In Oka et al. (eds.), Computer Methods and Advances in Geomechanics: 267-272. London: Taylor & Francis.

Monforte, L., Carbonell, J.M., Arroyo, M. & Gens, A. 2016. Performance of mixed formulations for the Particle Element Method in soil mechanics problems. *Computational Particle Mechanics* (in press).

Moss, R.E.S. 2014. A Critical State framework for seismic soil liquefaction triggering using CPT, *3rd International Symposium on Cone Penetration Testing, CPT14*, Las Vegas, Nevada, Paper 2#20.

Onate, E., Idelsohn, S.R., Del Pin, F. & Aubry, R. 2004. The particle finite element method an overview. *Int J Comput Meth*. 1:267–307.

O'Sullivan, C. 2011 *Particle-Based Discrete Element Modeling: A geomechanics perspective*. Hoboken, NJ: Taylor & Francis.

Randolph, M. F. 2004. Characterisation of soft sediments for offshore applications. *Proc. 2nd Int. Conf. Site Characterisation*, Porto 1: 209–232

Russell, A. R. & Muir Wood, D. 2009. Point load tests and strength measurments for brittle spheres. *I. J. of Rock Mech. and Mining Sciences*. 46: 272–280

Russell, A. R., Muir Wood, D. & Kikumoto, M. 2009. Crushing of particles in idealised granular assemblies. *J. Mech. Phys. Solids* 57: 1293–1313.
Schnaid, F. 2009. *In situ testing in geomechanics: the main tests*. London: Taylor & Francis.
Wesley L. D. 2007. Geotechnical characteristics of a pumice sand. In Tan et al. (ed.) *Characterisation and Engineering properties of Natural Soils*: 2449-2473. London: Taylor & Francis.
Zhang, X., Krabbenhoft, K., Pedroso D.M., Lyamin, A.V., Sheng, D., da Silva, M.V. & Wang, D. 2013. Particle finite element analysis of large deformation and granular flow problems. *Computers and Geotechnics*, 54: 133-142.
Zhang, X., Krabbenhoft, K., Sheng, D. & Li., W. 2015. Numerical simulation of a flow-like landslide using the particle finite element method. *Computational Mechanics*, 55: 167-177.

.